SUPPLEMENT TO THE *WELDING JOURNAL,* NOVEMBER 2009
Sponsored by the American Welding Society and the Welding Research Council

Al-to-Mg Friction Stir Welding: Effect of Positions of Al and Mg with Respect to the Welding Tool

The heat input and joint strength can be significantly affected by the positions of Al and Mg relative to the tool, and lap joint welding can be modified to double the joint strength

BY V. FIROUZDOR AND S. KOU

ABSTRACT

Dissimilar-metal welding has been identified as a top priority in materials joining technologies recently, such as welding Mg to Al or steel to reduce weight. Friction stir welding (FSW) is superior to fusion welding for joining dissimilar metals. Al-to-Mg FSW has been investigated frequently, but the basic issue of how the positions of Al and Mg with respect to the welding tool affect the joint strength is still not understood. In the present study, this issue was investigated in butt and lap FSW, and conventional lap FSW was modified to improve the joint strength. 6061 Al and AZ31 Mg, the two most widely used Al and Mg alloys, were selected. In butt FSW, Al was either on the advancing or retreating side of the tool with the tool shifted to Al, Mg, or neither. In lap FSW, on the other hand, Al was either at the top or bottom with deep or shallow pin penetration into the bottom. A significant effect of material position on the joint strength was demonstrated in butt, conventional lap, and modified lap FSW, affecting the joint strength by a factor of two or more. The highest joint strength in modified lap FSW doubled that in conventional dissimilar metal lap FSW and matched that in similar-metal lap FSW of AZ31 Mg to itself. How material position affects the heat input was predicted and confirmed by temperature measurements during FSW. A new color etching procedure was developed to show Al, Mg, Al_3Mg_2, and $Al_{12}Mg_{17}$ in different colors, clearly revealing the microstructure and material flow. The effect of material position on the heat input, material flow, and metallic bonding was used to explain how material position affects the joint strength. Increasing the heat input can increase liquation (i.e., liquid formation, even though FSW is solid-state welding) and hence cracking and brittle Al_3Mg_2 and $Al_{12}Mg_{17}$ to severely weaken the joint. The material position that reduces the heat input was suggested, which can be used to increase the joint strength as long as the heat input is still high enough for sufficient plastic material flow to prevent channels.

V. FIROUZDOR and S. KOU are, respectively, Graduate Student and Professor in the Department of Materials Science and Engineering, University of Wisconsin, Madison, Wis.

KEYWORDS

Aluminum
Butt Joint
Dissimilar Metals
Friction Stir Welding
Lap Joint
Magnesium

Introduction

The recent surveys conducted by the Joining and Welding Research Institute (JWRT) of Japan (Ref. 1) and the Edison Welding Institute (EWI) in the United States (Ref. 2) have both identified the welding of dissimilar metals as a top priority in materials joining technologies, for instance, Al to steel or Al to Mg for weight reduction, and Al to Cu for electric connections. Recently, friction stir welding (FSW) (Ref. 3) has been used to join dissimilar metals by plunging the pin at the bottom of a rotating tool into the workpiece and traversing it along the joint to cause metallic bonding by stirring and mixing the metals together.

Since Al and Mg alloys are both soft and similar in melting point, in an Al-to-Mg butt FSW, Al has been either on the advancing or retreating side of the rotating tool with tool offset to either Al or Mg. As for Al-to-Mg FSW of a lap joint, in the only study so far (Ref. 4), Al has been at the top but not the bottom. So, the effect of material position on the joint strength has not been studied in Al-to-Mg FSW in a lap joint.

Al-to-Mg FSW has been investigated frequently (Refs. 4–16) as shown in Table 1. In FSW of a butt joint Sato et al. (Ref. 10) and Zettler et al. (Refs. 12, 13) both found Mg on the advancing side better but not McLean (Ref. 5). McLean et al. (Ref. 5) and Yan et al. (Ref. 11) both found tool offset to Mg better. When the effect of material position on the joint strength was discussed, material flow, intermetallic compounds, and cracks were mentioned but not the heat input. In butt joint FSW without tool offset, Zettler et al. (Refs. 12, 13) observed higher peak temperatures when Al was on the advancing side. In double-pass FSW of a butt joint, Somasekharan et al. (Refs. 8, 9) observed complex intercalated microstructures in the stir zone with recrystallized lamellar-like shear bands rich in either Mg or Al. In Al-on-Mg FSW of a lap joint, Chen et al. (Ref. 4) kept the pin tip at an unspecified close distance above the Mg. Even though the pin never touched the Mg, a thick "conversion zone" containing brittle intermetallic compounds ($Al_{12}Mg_{17}$, Al_3Mg_2, and Mg_2Si) still existed between the stir zone and Mg to weaken the joint.

The present study investigates the effect

Table 1 — FSW of Al Alloys to AZ31 Mg

	Al Alloy	Butt Joint		Lap Joint		Welding Parameters
		Advancing Side	Tool Offset	Top	Pin Tip	
McLean (Ref. 5)	5083 Al	Al (visually better), Mg	Mg (visually better), Al			300–400 rev/min 60–100 mm/min
Hirano (Ref. 6)	1050 Al	unspecified	unspecified			1500–3000 rev/min 200–800 mm/min
Okamura (Ref. 7)	1050 Al	Mg	none			unspecified
Somasekharan (Refs. 8, 9)	6061 Al	Al, Mg	Al, Mg			800 rev/min 90 mm/min
Sato (Ref. 10)	1050 Al	Al (failed), Mg (didn't)	none			2450 rev/min 90 mm/min
Yan (Ref. 11)	1060 Al	Al	Mg (strongest), Al, none			200–1000 rev/min 19–75 mm/min
Zettler (Refs. 12, 13)	6040 Al	Mg (stronger), Al	none			1400 rev/min 200–225 mm/min
Kwon (Ref. 14)	5052 Al	Al	none			800–1600 rev/min 300 mm/min
Kostka (Ref. 15)	6040 Al	Al	none			1400 rev/min 225 mm/min
Liu (Ref. 16)	2024 Al	Al	none			2500 rev/min 45 mm/min
Chen (Ref. 4)	Al-7.5Si			Al	above Mg	1500 rev/min 20–80 mm/min

Table 2 — Composition of Workpiece Materials (wt-%)

	Si	Cu	Mn	Mg	Cr	Zn	Ti	Fe	Al
6061 Al	0.62	0.28	0.08	0.89	0.19	0.02	0.01	0.52	bal
AZ31	—	—	0.5	bal	—	1.0	—	—	3.0

of material position on the heat input, material flow, and joint strength in Al-to-Mg FSW, considering the effect of the heat input on intermetallic compounds, and cracks in butt joint welding, conventional lap joint welding (both single- and dual-pass), and modified lap joint welding (both single- and dual-pass). In view of the large number of combinations, the travel speed and the rotation speed were fixed in order to focus on the effect of material position. The effect of the travel and rotation speeds will be discussed in a follow-up paper elsewhere.

Experimental Procedure

6061 Al was welded to AZ31B Mg by FSW. Their nominal chemical compositions are listed in Table 2. As a reference for comparison, AZ31 Mg was welded to itself and so was 6061 Al. Coupons were cut from 1.6-mm-thick sheets of AZ31 Mg alloy and 6061-T6 Al alloy. They were cleaned with a stainless steel brush to remove surface oxides. A Lagun FTV-1 milling machine (2.2 kW or 3 hp) was used for FSW with tools prepared from a H13 tool steel. The tool shoulder was 10 mm in diameter and concave. The pin was 4 mm in diameter and threaded. For welding of the butt joint, the pin length was 1.3 mm. For lap joint welding, both conventional and modified, the pin length was 1.5 mm. Additional conventional lap joint welding was also conducted with a longer pin length of 2.3 mm. The tool was rotated counterclockwise when viewed from above, and tilted 3 deg forward. The workpieces were clamped down tight with four steel fingers located 10 mm away from the weld interface. The tool was cleaned after each welding pass by plunging into a fresh piece of 6061 Al, which removed the material stuck on the tool from previous welds.

Two different rotation speeds, 1400 and 800 rev/min, were used initially. Except for one weld, the joint strength was significantly lower with 800 rev/min. The rotation speed was fixed at 1400 rev/min in all subsequent experiments. The travel speed was 38 mm/min.

Butt Joint Welding

The workpiece dimensions are shown in Fig. 1A. The welding conditions are listed in Table 3. AZ31 Mg was either on the advancing or retreating side of the tool. The tool axis was positioned along the joint (no offset) or shifted 1.5 mm (1.5 mm offset) to either 6061 Al or AZ31 Mg.

Lap Joint Welding

The workpiece dimensions are shown in Fig. 1B. The welding conditions are listed in Table 4. The weld in the lap joint was positioned along the centerline of the 38-mm-wide overlap. Conventional dual-pass welding of the lap joint was similar in material position except that a second pass was made from the opposite side such that its centerline was 10 mm away from the centerline of the first pass. The purpose was to determine how much the joint strength could be increased by making a second pass. The welding conditions are listed in Table 5.

Single-pass modified lap joint welding is shown in Fig. 1C and the welding conditions in Table 6. A small piece of the bottom sheet material, 76 mm long, 19 mm wide, and 1.6 mm thick, was butt joint welded to the top sheet with pin penetration into the bottom sheet. The 19-mm width of the small piece was mainly for the space required for clamping instead of welding. When AZ31 Mg was on the top, whether it was the top sheet or the small piece, it was placed on the advancing side of the tool. This was because, as will be shown subsequently, butt joint welds were significantly weaker with 6061 Al on the advancing side. Modified dual-pass lap joint welding was similar in material position except a second pass was made from the opposite side, again with its centerline 10 mm away from that of the first pass. The welding conditions are listed in Table 7.

Tensile Testing

The joint strength was determined by tensile testing normal to the weld. Welded coupons were cut in the direction normal to the weld into 12-mm-wide tensile specimens. The edges of the tensile specimens were polished smooth with 320-grit grinding paper. For lap joint welds, a 1.6-mm-thick sheet was placed at each end of the tensile specimen to initially align the specimen with the loading direction. A Sintech tensile testing machine was used, and the speed of the crosshead movement was 1 mm/min. Two to four specimens from welds made under the same condition were tested.

Temperature Measurements

A computer-based data acquisition system was used along with K-type thermocouples for temperature measurements at 100 Hz during FSW. The thermocouple, with a stainless steel sheath of 0.5 mm outer diameter, was placed in a 0.5 × 0.5 mm groove at the workpiece surface that ends 3 mm away from the path of the tool axis. In FSW of both conventional and modified lap joints, the grooves were at the top surface of the lower sheet. In FSW of the butt joint, on the other hand, they were at the bottom surface of the workpiece.

Weld Microstructure

Transverse weld cross sections were prepared by polishing and etching in three steps. The first step was to etch the samples with a solution consisting of 10 mL acetic acid, 10 mL distilled water, and 6 g picric acid in 100 mL ethanol for 10 s (to reveal the AZ31 part of the microstructure). The second step was to etch them with a solution consisting of 20 g NaOH in 100 mL distilled water for 40 s (to reveal the grain structure in 6061 Al). The final step was to dip them in a solution consisting of 4 g $KMnO_4$ and 2 g NaOH in 100 mL dis-

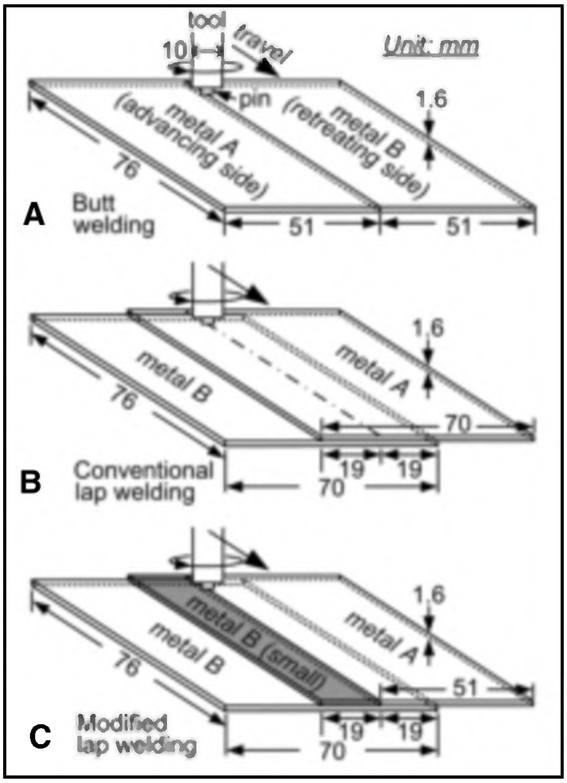

Fig. 1 — Friction stir welding of metal A to metal B. A — Butt joint; B — conventional lap joint; C — modified lap joint (butt joint welding a small piece of metal B to metal A with pin penetration into bottom metal B). Advancing side — material pushed forward by tool; retreating side — material pushed backward.

Table 3 — Welds in Butt Joint

#	Joint	Rotation Speed (rev/min)	Travel Speed (mm/min)	Pin Length (mm)	Tool Offset (mm)	Tensile Load (N)	Standard Deviation (±N)
B-1	Al to Al	1400	38	1.3	0	3109	19
B-2	Mg to Mg	1400	38	1.3	0	2580	102
B-3	Mg (ret) to Al (adv)	1400	38	1.3	0	1318	249
B-4	Al (ret) to Mg (adv)	800	38	1.3	0	1337	247
B-5	Al (ret) to Mg (adv)	1400	38	1.3	0	2055	274
B-6	Al (ret) to Mg (adv)	800	38	1.3	1.5 into Mg	2590	73
B-7	Al (ret) to Mg (adv)	1400	38	1.3	1.5 into Mg	2109	217
B-8	Al (adv) to Mg (ret)	1400	38	1.3	1.5 into Mg	<400	—
B-9	Al (ret) to Mg (adv)	800	38	1.3	1.5 into Al	<400	—
B-10	Al (ret) to Mg (adv)	1400	38	1.3	1.5 into Al	1589	—
B-11	Mg (ret) to Al (adv)	1400	38	1.3	1.5 into Al	<400	—

Table 4 — Single-Pass Welds in a Conventional Lap Joint

#	Joint	Rotation Speed (rev/min)	Travel Speed (mm/min)	Pin Length (mm)	Tensile Load (N)	Standard Deviation (±N)
CL-5	Al to Al	1400	38	1.5	3356	54
CL-6	Mg to Mg	1400	38	1.5	2463	190
CL-1	Al (top) to Mg (bottom)	1400	38	1.5	862	25
CL-2	Mg (top) to Al (bottom)	1400	38	1.5	1077	6
CL-3	Al (top) to Mg (bottom)	1400	38	2.3	554	5
CL-4	Mg (top) to Al (bottom)	1400	38	2.3	978	90

Table 5 — Dual-Pass Welds in a Conventional Lap Joint

#	Joint	Rotation Speed (rev/min)	Travel Speed (mm/min)	Pin Length (mm)	Tensile Load (N)	Standard Deviation (±N)
CL-7	Top: Mg and 1st pass; Bottom: Al and 2nd pass	1400	38	1.5	2269	31

Table 6 — Single-Pass Welds in a Modified Lap Joint

#	Joint	Rotation Speed (rev/min)	Travel Speed (mm/min)	Pin Length (mm)	Tool Offset at Top	Tensile Load (N)	Standard Deviation (±N)
ML-5	Top: Al (ret) and small Mg (adv); Bottom: Mg	800	38	1.5	1.5 into small Mg	1808	8
ML-1	Top: Al (ret) and small Mg (adv); Bottom: Mg	1400	38	1.5	1.5 into small Mg	2711	235
ML-2	Top: Mg (adv) and small Al (ret); Bottom: Al	1400	38	1.5	1.5 into small Al	1434	14
ML-3	Top: Mg (adv) and small Al (ret); Bottom: Al	1400	38	1.5	0	993	98
ML-4	Top: Al (ret) and small Mg (adv); Bottom: Mg	1400	38	1.5	0	1797	136

tilled water for 10 s (to make Al colorful). A 2-step etching procedure was used by Somasekharan et al. (Ref. 9) for color metallography of butt joint welds between AZ91D Mg and 6061 Al. The 3-step etching procedure showed Al, Mg, Al_3Mg_2, and $Al_{12}Mg_{17}$ all in different colors.

A JEOL JSM-6100 scanning electron microscope with energy-dispersive spectroscopy (EDS) was used for chemical composition measurements. A Hi-Star 2-D X-ray diffractometer with an area detector was used to identify the intermetallic compounds.

Results and Discussion

The experimental results are summarized in Tables 3–7. Due to space limitations, the microstructure of six representative welds will be shown here. The remaining welds will be shown elsewhere.

Al-Mg Phase Diagram

For convenience of discussion, the binary Al-Mg phase diagram (Ref. 17) is shown in Fig. 2. There are two eutectics. The first one is between the Al-rich phase

(Al) and Al_3Mg_2, which is essentially Al_3Mg_2, and the second between the Mg-rich phase (Mg) and $Al_{12}Mg_{17}$. Both eutectic temperatures, 450°C for the former and 437°C for the latter, are far below the melting points of Al (660°C) and Mg (650°C).

According to the Al-Mg phase diagram shown in Fig. 2, when Al and Mg are heated together such as during FSW, intermetallic compounds Al_3Mg_2 and $Al_{12}Mg_{17}$ can form, the former on the Al side and the latter on the Mg side. Upon further heating, the eutectic reaction Mg + $Al_{12}Mg_{17} \rightarrow L$ occurs at the eutectic temperature 437°C and the eutectic reaction Al + $Al_3Mg_2 \rightarrow L$ at the eutectic temperature 450°C. This liquid formation is called constitutional liquation (Refs. 10, 18–21). At room temperature Al_3Mg_2 contains about 37 wt-% Mg and $Al_{12}Mg_{17}$ about 57 wt-% Mg. The eutectic temperatures 437° and 450°C are more than 200°C below the melting point of either Al or Mg, and they can be reached easily during Al-to-Mg FSW to form liquid films along the interface between Al and Mg. Upon cooling, the two eutectic reactions are reversed, and Al_3Mg_2 and $Al_{12}Mg_{17}$ form from the liquid L.

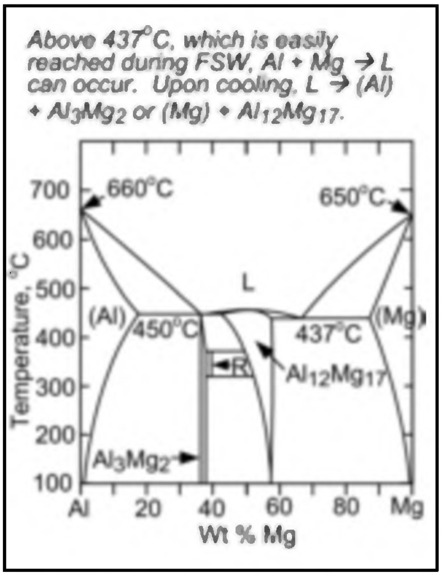

Fig. 2 — Al-Mg phase diagram (Ref. 17) explaining liquid formation (i.e., liquation) in Al-to-Mg FSW.

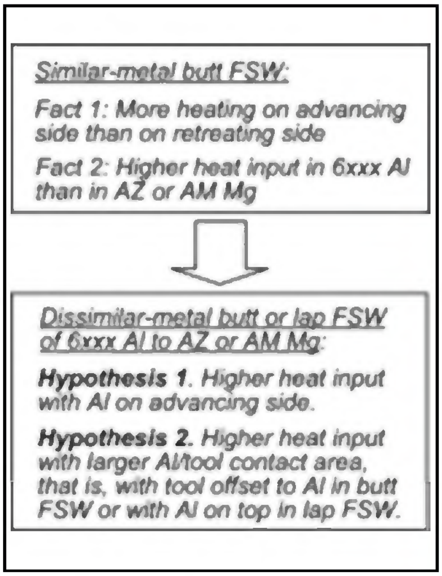

Fig. 3 — Hypotheses on heat input in FSW between 6xxx Al alloy and AZ (Mg-Al-Zn) or AM (Mg-Al-Mn) Mg alloy.

Hypotheses on Heat Input in FSW

In order to explain the effect of material position on the joint strength, the effect of material position on the heat input will be discussed first. This is because liquation increases with increasing heat input (Ref. 20). The more liquation becomes, the more liquid films can form along grain boundaries and, in the case of Al-to-Mg FSW, the Al/Mg interface. Since the liquid films weaken the Al/Mg interface, cracking can occur along the interface under the shearing force by the tool.

Figure 3 shows two hypotheses made based on two facts regarding the heat input in FSW. Fact 1 is as follows: In similar-metal butt joint FSW, more heating occurs on the advancing side than the retreating side. Both computer simulations and temperature measurements (Refs. 22–25) have shown higher peak temperatures on the advancing side. As mentioned previously, the advancing side is the side where material is pushed forward by the rotating tool, while the retreating side is the side where material is pushed backward. Using FSW with a milling machine as an example, the rotating tool is stationary and the workpiece material "flows" in the direction opposite to the welding direction. On the advancing side, the tool rotates in the opposite direction of workpiece flow, while on the retreating side it rotates in the same direction. Consequently, the material on the advancing side tends to experience greater shearing and heating than that on the retreating side.

For a lower conductivity material such as 304 stainless steel, as pointed out by Nandan et al. (Ref. 23), the temperature on the advancing side can be as much as 100°C higher than on the retreating side. For a higher conductivity material such as an Al or Mg alloy, the difference is smaller. However, the liquation (eutectic) temperatures are rather low (437° and 450°C). Furthermore, a relatively small temperature increase can significantly increase the fraction of liquid, that is, the extent of liquation. For instance, according to the Al-Mg phase diagram (Fig. 2), a material with 60 wt-% Mg and 40 wt-% Al has a melting temperature range of only about 10°C. Thus, this material begins to liquate at the eutectic temperature 437°C and melts completely at about 447°C.

Fact 2 is as follows: In similar-metal butt joint FSW, more heating occurs in 6xxx Al alloys than in AZ (Mg-Al-Zn) or AM (Mg-Al-Mn) Mg alloys. In similar-

Table 7 — Dual-Pass Welds in a Modified Lap Joint

#	Joint	Rotation Speed (rev/min)	Travel Speed (mm/min)	Pin Length (mm)	Tool Offset (mm)	Tensile Load (N)	Standard Deviation (±N)
ML-6	Top: Al (ret) and small Mg (adv); Bottom: Mg (adv) and small Al (ret)	1400	38	1.5	1.5 into small Mg and small Al	4530	87
ML-7	Top: Al (ret) and small Mg (adv); Bottom: Mg (adv) and small Al (ret)	1400	38	1.5	0	3559	116

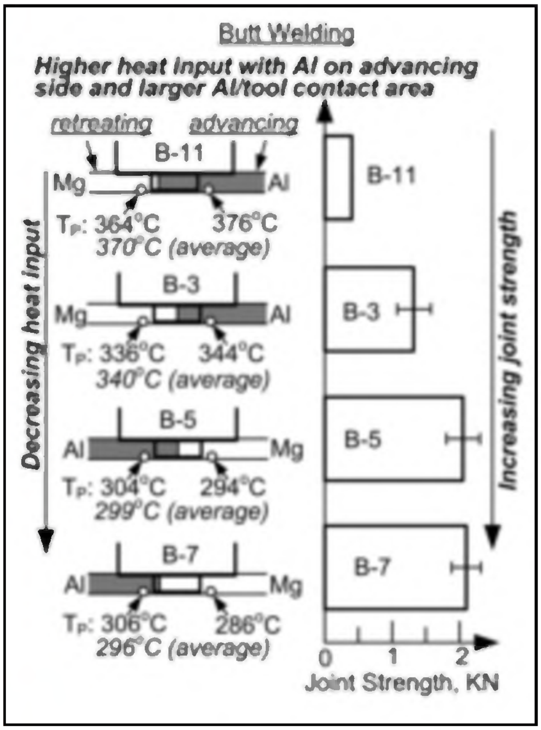

Fig. 4 — Effect of material position on joint strength and heat input in butt joint FSW of AZ31 Mg and 6061 Al. The thermocouples are 3 mm away from the path of the tool axis and 0.25 mm above the bottom surface of the workpiece.

metal butt joint FSW, Zettler et al. (Ref. 12) observed higher peak temperatures (100°C higher on the advancing side and 80°C on the retreating side, both at 10 mm from the joint line) in 6040 Al than in AZ31 Mg. Similar trends have been observed in the following three studies on similar-metal friction stir spot welding (FSSW), where heat is generated by a rotating but stationary tool. Gerlich et al. (Ref. 26) observed in the stir zone at the tool shoulder a higher peak temperature (about 80°C higher) in 6111 Al than in AZ91 Mg. Su et al. (Ref. 27) observed a higher torque and heat input (almost three times higher heat input) in 6061 Al than in AM60 Mg. Yang et al. (Ref. 21) observed a higher torque and heat input (twice higher heat input) in 6061 Al than in AZ91 Mg.

Fact 2, perhaps, can be further explained as follows. First, Yang et al. (Ref. 21) have shown in similar-metal FSSW that AZ and AM Mg can liquate much more easily than 6xxx Al. In AZ and AM Mg (and most other Mg alloys because Al is the most widely used alloying element in Mg alloys) $Al_{12}Mg_{17}$ is present to react with the surrounding Mg-rich matrix to form liquid at 437°C — Fig. 2. The liquid films at interface between the tool and the stir zone can cause tool slippage, while those along grain boundaries within the stir zone can decrease its resistance to tool rotation. Consequently, the torque and the work it does, which contributes to nearly all of the heat input, are significantly lower in welding AZ and AM Mg than 6xxx Al (Refs. 21, 27). Second, with its face-centered cubic (fcc) structure, Al has more slip planes available for deformation than Mg, which is hexagonal close-packed (hcp) in structure. Thus, as compared to Mg, Al is more deformable. Zettler et al. (Ref. 12) noted in similar-metal butt joint FSW that the stir zone was twice as big in cross section in 6040 Al than in AZ31 Mg, which perhaps suggests more heating by viscous dissipation in the former. Maybe computer simulation can show if heat generation is higher in 6061 Al or AZ31 Mg.

Based on the two facts, two hypotheses can be made regarding dissimilar-metal FSW of 6xxx Al to AZ or AM Mg with the same tool at the same rotation speed and travel speed. Hypothesis 1 is as follows: A higher heat input can be expected in FSW of the butt joint with Al on the advancing side. Hypothesis 2 is as follows: A higher heat input can be expected with a larger Al/tool contact area. A larger Al/tool contact area can exist in the following two cases: first, with tool offset to Al in butt joint FSW and, second, with Al on the top in lap joint FSW. Regarding the first case, the difference can be expected to be more significant with Al on the advancing side in view of Hypothesis 1. These hypotheses will be used subsequently to explain the effect of material position on the heat input in Al-to-Mg FSW.

Butt Joint Welding

The effect of material position on the joint strength in butt joint FSW is shown in Fig. 4. First, material position has a significant effect on the joint strength; the difference can be a factor of four. Second, the joint strength is higher with AZ31 Mg on the advancing side. Third, increasing tool offset to AZ31 Mg improves the joint strength (the three butt welds in Table 2 made at 800 rev/min show the same trend).

As shown in Table 1, Sato et al. (Ref. 10) and Zettler et al. (Ref. 12) both found AZ31 Mg on the advancing side better, which is consistent with the present study. Both McLean et al. (Ref. 5) and Yan et al. (Ref. 11) found tool offset to AZ31 Mg better, which is also consistent with the present study except AZ31 Mg was put on the retreating side by Yan et al. (Ref. 11).

Based on the two hypotheses mentioned previously, with the same tool at the same rotation speed and travel speed, the effect of material position on the heat input in Al-to-Mg butt joint FSW can be predicted as shown by the arrow indicating the direction of decreasing heat input in Fig. 4. First, the heat input can be higher in FSW of the butt joint with Al on the advancing side (welds B-11 and B-3) than with Al on the retreating side (welds B-5 and B-7). Second, with Al on the advancing side, the heat input can be higher with tool offset to Al (weld B-11) than without any offset (weld B-3). Third, the heat input can be lower with tool offset to Mg (weld B-7) than without any offset (weld B-5), but the difference is likely smaller because Al is on the retreating side.

As shown in Fig. 4, the measured peak temperatures are in agreement with the prediction. The thermocouples were 3 mm away from the path of the tool axis and 0.25 mm above the bottom surface of the workpiece. As mentioned previously, in butt joint FSW of 6040 Al to AZ31 Mg without tool offset, Zettler et al. (Ref. 12) observed higher peak temperatures (50°C higher on the advancing side and 30°C on the retreating side) with 6040 Al on the advancing side, which are consistent with welds B-3 and B-5 in Fig. 4. Although these higher peak temperatures were not explained or used to explain the joint strength, the study of Zettler et al. (Ref. 12) was very interesting and shed much light for the present study.

Figure 5 compares the thermal cycles measured in welds B-7 and B-11. In weld B-11, where Al is on the advancing side, the peak temperature is 376°C on the advancing side and 364°C on the retreating side, the average being 370°C. In weld B-7, where Mg is on the advancing side, the peak temperature is 286°C on the advancing side and 306°C on the retreating side, the average being 296°C, which is 74°C lower than the average peak temperature of 370°C in weld B-11. In similar-metal butt joint FSW, as mentioned previously, the peak temperature is higher on the advancing side. However, weld B-7 (and weld B-5 as well) shows that this can be reversed in a FSW dissimilar-metal butt joint.

Now the effect of material position on the heat input can be compared with the effect of material position on the joint strength to see if they correlate with each other. As shown in Fig. 4, weld B-11 is significantly weaker than weld B-3, weld B-3 is significantly weaker than weld B-5, and weld B-5 is similar to weld B-7 in strength. A similar pattern exists in the measured average temperatures. Thus, a close correlation seems to exist between increasing heat input and decreasing joint strength. It is well known that the extent of liqua-

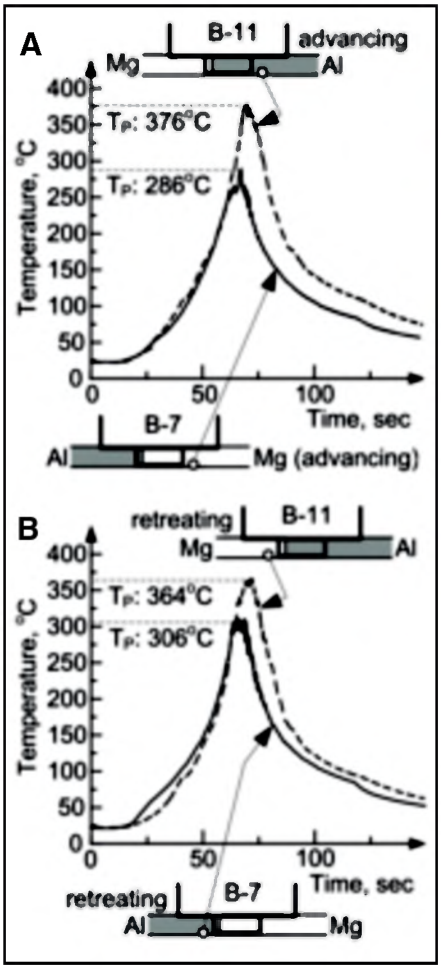

Fig. 5 — *Thermal cycles measured for welds B-7 and B-11 in butt joints. The thermocouples are 3 mm away from the path of the tool axis and 0.25 mm above the bottom surface of the workpiece.*

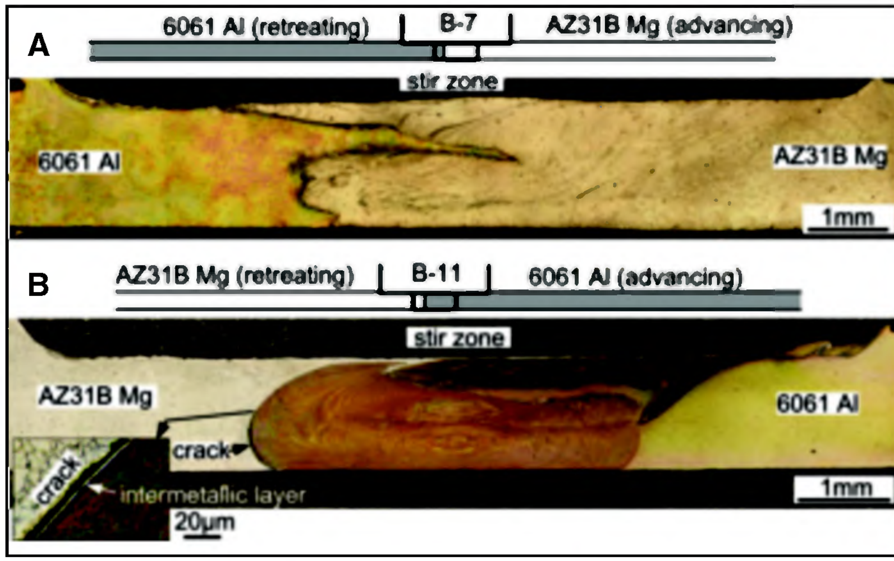

Fig. 6 — *Transverse cross sections of welds in butt joints. A — Weld B-7; B — weld B-11.*

tion increases with increasing heat input or temperature (Ref. 20). With more liquation, more liquid can form along the Al/Mg interface to promote cracking under the shearing action of the tool and form brittle intermetallics both along the interface and grain boundaries inside the stir zone upon cooling. The joint strength can be significantly reduced.

Although Fig. 4 can explain how material position can affect the joint strength through the heat input and hence liquation, other factors may also affect the joint strength. For instance, interlocking between Mg and Al can improve the joint strength, so can similar-metal bonding (such as Al-to-Al and Mg-to-Mg, as will be shown subsequently in modified lap welding). On the other hand, excessive mixing between Al and Mg can provide more interface area for Al to react with Mg to cause liquation and decrease the joint strength.

Figure 6 compares the transverse cross sections of welds B-7 and weld B-11. The Al/tool contact area in weld B-7 is the same as the Mg/tool contact area in weld B-11. In weld B-7 Al penetrates deep into the stir zone, which can promote interlocking and improve the joint strength. However, there is no Mg penetration into the stir zone in weld B-11. In fact, a long open crack exists along the interface between Mg and the stir zone over half the thickness of the workpiece. There might be two reasons for the differences. First, with its good deformability Al can move to the back of the rotating tool from the retreating side even though shearing is less there than the advancing side. Zhang (Ref. 28) has shown by computer simulation that material particles at the advancing side can enter into the retreating side but not the other way around. With its lower deformability, however, Mg is less able to move far away from the retreating side. Second, the higher heat input and hence liquation in weld B-11 could have caused a continuous liquid film to exist along the interface between Mg and the stir zone over half the thickness of the workpiece. The slippage caused by the liquid film could have kept Mg from being dragged deep into the stir zone. The large open crack and the continuous intermetallic layer along the interface both suggest liquation there. The crack caused weld B-11 to break even before tensile testing. Thus, lack of interlocking caused by unfavorable material flow and more liquation caused by the higher heat input could have both contributed to the low joint strength of weld B-11.

The microstructure of weld B-3 (to be shown elsewhere due to space limitations) indicated heavy liquation within the stir zone due to relatively high heating and excessive mixing between Al and Mg caused by zero offset (equal volume of Al and Mg exposed to the pin).

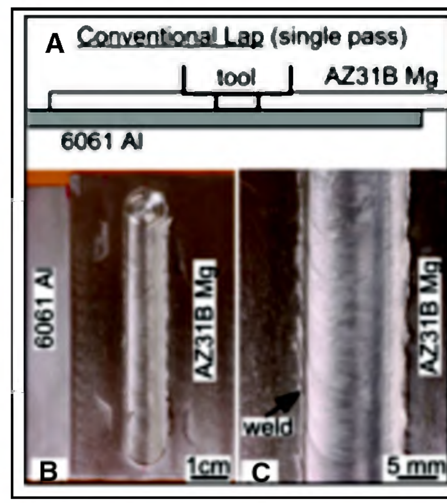

Fig. 7 — *Single-pass weld in a conventional lap joint (CL-2) with AZ31 Mg on top of 6061 Al. A — Material position; B — top view overall; C — top view enlarged.*

Single-Pass Conventional Lap Joint

Figure 7 shows a single-pass weld in a conventional lap joint with AZ31 Mg on the top (CL-2). The effect of material position on the joint strength is shown in Fig. 8. First, material position has a significant effect on the joint strength. The difference can be a factor of two. Second, the strength is higher with AZ31 Mg on the top. Third, the strength is higher with the 1.5-mm pin length than with 2.3 mm. Fourth, for dissimilar-metal FSW between AZ31 Mg and 6061 Al, the highest strength in a conventional lap joint weld (CL-2) is much lower than that in a butt joint weld (B-7 in Fig. 4), only about one half. Butt joint welds are stronger mainly because lap joint welds are subjected to shearing/peeling forces during tensile testing, while butt joint welds are not.

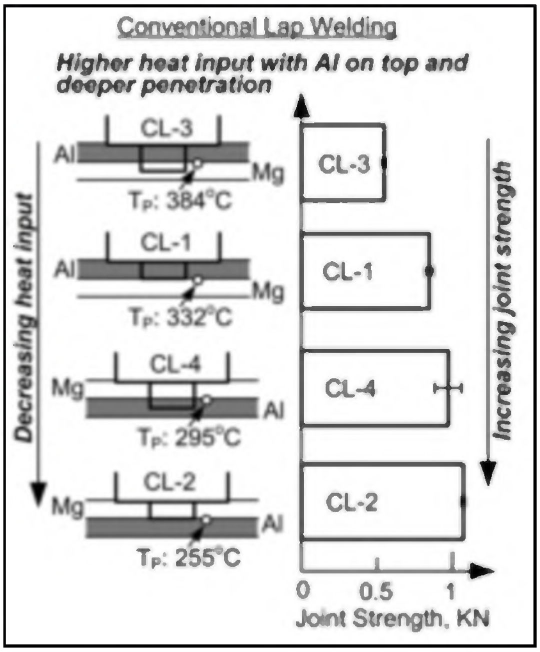

Fig. 8 — Effect of material position on joint strength and heat input in conventional lap joint FSW of AZ31 Mg and 6061 Al. The thermocouples are 3 mm away from the path of the tool axis and 0.25 mm below the top surface of the lower sheet.

travel speed, a higher heat input can be expected with a larger Al/tool contact area, that is, with 6xxx Al on the top to increase the Al/tool contact area. Thus, a higher heat input can be expected in welds CL-3 and CL-1 than in welds CL-4 and CL-2. With a longer pin penetrating into the lower sheet, a higher heat input can be expected in weld CL-3 than weld CL-1 and in weld CL-4 than weld CL-2.

To verify that the heat input is higher with Al on the top and with a longer pin, temperature measurements were conducted. The thermocouples were located 3 mm away from the path of the tool axis and 0.25 mm below the top surface of the lower sheet. As shown in Fig. 8, the peak temperature is 77°C higher with 6061 Al on the top (weld CL-1) than at the bottom (weld CL-2). Thus, this confirms the higher heat input in Al-to-Mg lap joint FSW is with Al on the top. Furthermore, the peak temperatures are higher with a longer pin, that is, 52°C higher in weld CL-3 than CL-1 and 40°C higher in weld CL-4 than CL-2. The authors are unaware of any similar data for lap joint FSW published previously. The data of Gerlich et al. (Ref. 26) were for FSSW of 6111 Al to AZ91 Mg, where the peak temperature measured in the stir zone near the tool shoulder was about 90°C higher with 6111 Al at the top. Since no tensile testing was conducted by Gerlich et al. (Ref. 26), the temperature measurement was not used to explain the effect of material position on the joint strength.

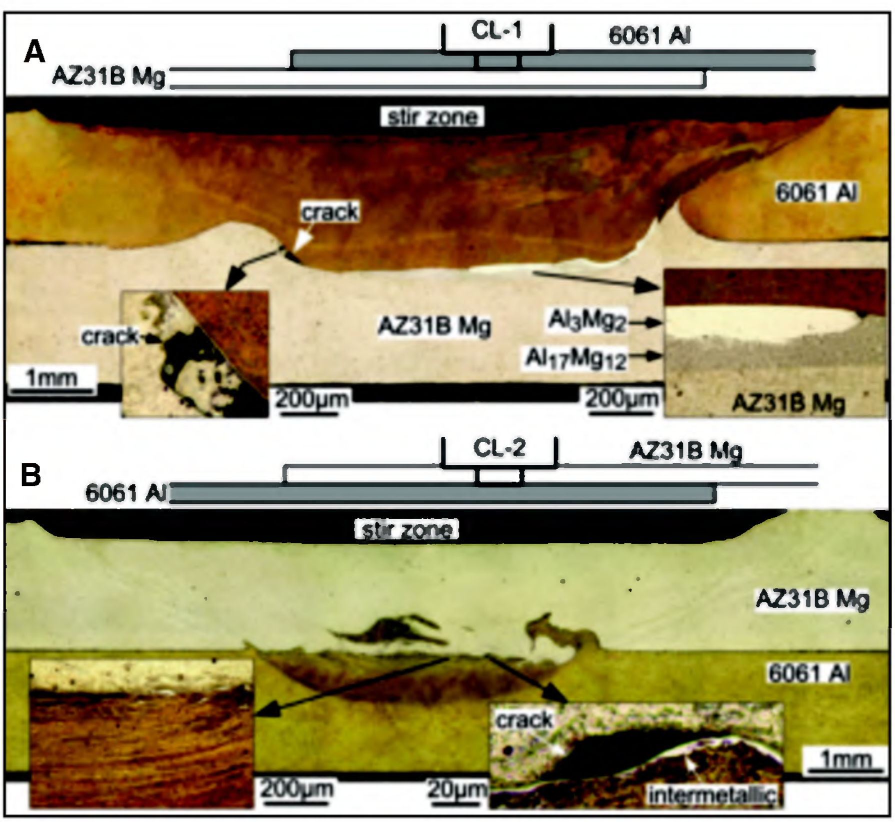

Fig. 9 — Transverse cross sections of welds in conventional lap joints. A — Weld CL-1; B — weld CL-2.

The effect of material position on the heat input in conventional lap joint FSW of 6xxx Al to AZ or AM Mg is predicted in Fig. 8. According to Hypothesis 2, with the same tool at the same rotation speed and

Figure 9 shows the transverse cross sections of welds CL-1 and CL-2. In weld CL-1 (Fig. 9A) thick intermetallic compounds and a crack are present along the interface between the Al stir zone and AZ31 Mg at the bottom. The brittle intermetallics and crack must have contributed to the low joint strength of the weld. As mentioned previously, in lap joint FSW Chen et al. (Ref. 4) observed a very thick layer of intermetallics at the interface between Al-7.5Si (top) and AZ31 Mg (bottom) even though the pin never touched AZ31 Mg. Thus, slight or no pin penetration into AZ31 Mg does not really matter much. Instead, putting AZ31 Mg on the top might work better (as shown by weld CL-2).

Energy-dispersive X-ray (EDX) analysis showed the lighter layer next to 6061 Al (inset on right) contained about 39 wt-% Mg, which is close to the 37 wt-% Mg for Al_3Mg_2. The darker layer next to AZ31 Mg contained about 63 wt-% Mg, which is reasonably close to the 57 wt-% Mg for $Al_{12}Mg_{17}$. Electron probe microanalysis (EPMA) confirmed the compositions. X-ray diffraction (XRD) also confirmed the presence of $Al_{12}Mg_{17}$ and Al_3Mg_2. This is consistent with the report of Liu et al. (Ref. 29) on an Al/Mg diffusion couple annealed at 420°C for 4 h. By EPMA and the Al-Mg phase diagram, they identified an Al_3Mg_2 sublayer on the Al side and an $Al_{12}Mg_{17}$ sublayer on the Mg side.

The intermetallic layers in weld CL-1 (Fig. 9A) suggest that heating during FSW was high enough to cause Al and Mg to react with each other and form liquid along the interface, that is, constitutional liquation. The Mg near the Al stir zone does not appear to be stirred (no flow lines visible in AZ31 Mg in inset on right), possibly because of the lower deformability of Mg or tool slippage by liquid films formed by liquation or both. Upon cooling, $Al_{12}Mg_{17}$ and Al_3Mg_2 formed from the liquid by eutectic reactions — Fig. 2.

EDX showed the particle inside the crack at the interface (inset on left in Fig. 9A) contained about 60 wt-% Mg, close to the 57 wt-% Mg of $Al_{12}Mg_{17}$. This suggests that liquation occurred here and the liquid film caused the stir zone to be separated from AZ31 Mg under shearing by the rotating tool. It is worth mentioning that in FSW cavities can form in the stir zone by material flow without liquation. With a longer pin (2.3 mm instead of 1.5

mm) to penetrate deeper into AZ31 Mg, that is, in weld CL-3, much more intermetallics formed at the interface near the pin tip due to more heating (52°C higher peak temperature as shown in Fig. 8). Due to space limitations, the microstructure will be shown elsewhere.

In weld CL-2 (Fig. 9B) the intermetallics are thinner and cracks smaller and shorter along the interface between the Mg stir zone and the 6061 Al at the bottom. The region of 6061 Al next to the Mg stir zone appears to be well stirred (flow lines visible in inset on left). All these suggest that, as compared to weld CL-1, liquation was significantly less, consistent with the lower heat input in weld CL-2 (77°C lower peak temperature as shown in Fig. 8). With a longer pin to penetrate deeper into 6061 Al than in weld CL-2, that is, in weld CL-4, more cracks and intermetallics formed at the interface near the pin tip due to more heating (40°C higher peak temperature as shown in Fig. 8). Due to space limitations, the microstructure will be shown elsewhere.

Single-Pass Weld in Modified Lap Joint

In order to improve the strength of Al-to-Mg welds, a conventional lap joint was modified. Figure 10 compares FSW of dissimilar metals A and B in a conventional lap joint with the proposed modified lap joint. With conventional lap joint welding (Fig. 10A), metal A is placed on top of metal B. As mentioned previously, with only slight or even no pin penetration into metal B, metals A and B can still react with each other and form a rather thick layer of intermetallics at the interface. With the modified lap joint (Fig. 10B), metal A is still placed on top of metal B but with a small piece of metal B next to it. With tool offset to the small piece B, weak A-to-B lap joint FSW can be minimized and stronger A-to-A or B-to-B lap joint FSW can be maximized. Metal A can be 6061 Al and metal B AZ31 Mg or vice versa.

Figure 11 shows a single-pass modified lap joint weld with AZ31 Mg and a small piece of 6061 Al at the top (ML-2). As mentioned previously (Fig. 10), modified lap joint welding involves both butt and lap joint welding. In light of the butt joint welding result (Fig. 4), all welds were made with AZ31 Mg on the advancing side, either as the top sheet or the small piece at the top.

The effect of material position on the joint strength in single-pass FSW in the modified lap joint is shown in Fig. 12. First, material position has a significant effect on the joint strength, and the difference can be a factor of two to three. Second, the strength is highest in the weld (ML-1) with a tool offset to the small piece of AZ31 Mg. This is consistent with

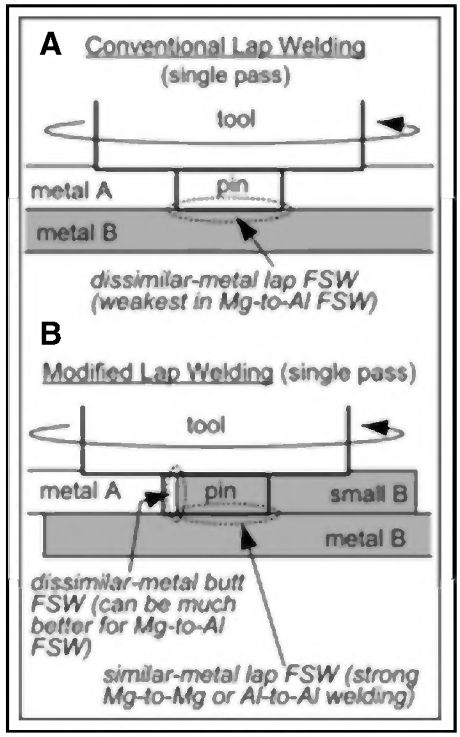

Fig. 10 — Single-pass FSW of metal A to metal B in a lap joint. A — Conventional lap joint; B — modified lap joint (by butt joint welding a small piece of metal B to metal A with pin penetration into bottom metal B).

the butt joint welding result — Fig. 4. This also allows much Mg-to-Mg lap joint welding, which is much stronger than Al-to-Mg lap joint welding because of the absence of cracks and intermetallics. Third, weld ML-1 (2,711N) matched in strength the similar-metal lap joint weld CL-6 (2,463N as shown in Table 3) between AZ31 Mg and itself.

Figure 13 compares the tensile test curves of the best single-pass conventional lap joint weld CL-2 and the best single-pass modified lap joint weld ML-1. Weld ML-1 failed at a significantly higher strength and elongation than weld CL-2.

The effect of material position on the heat input with a FSW in a modified lap joint is predicted in Fig. 12. According to Hypothesis 2, with the same tool at the same rotation speed and travel speed, a higher heat input can be expected with a larger Al/tool contact area. Since the contact area between Al and the tool (shoulder and pin) decreases in the order of ML-2, ML-3, ML-4, and ML-1, the heat input can be expected to decrease in the same order. This prediction is confirmed by the peak temperatures measured during FSW. The thermocouples were on the advancing side and located 3 mm away from the path of the tool axis and 0.25 mm below the top surface of the lower sheet. Going from weld ML-3 to weld ML-4, the bottom sheet changes from 6061 Al to AZ31 Mg, which is lower in thermal con-

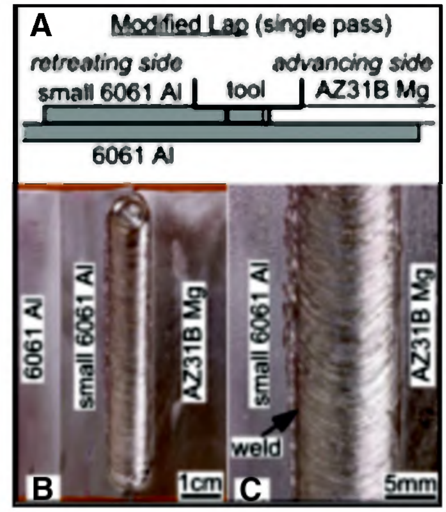

Fig. 11 — Single-pass weld in a modified lap joint (ML-2) with AZ31 Mg on top of 6061 Al. A — Material position; B — top view overall; C — top view enlarged.

ductivity (167 vs. 96 W/m°C). The fact that the peak temperature still decreases suggests the effect of thermal conductivity difference is not very significant.

Figure 14 shows the transverse cross sections of welds ML-3 and ML-1. In weld ML-3 (Fig. 14A) Al and Mg interpenetrate deep into each other, and this can be expected to promote interlocking and improve the joint strength. Unfortunately, the heat input was relatively high (Fig. 12), and it caused much liquation and a long crack along most of the Mg-Al interface (see insets). Under the shearing/peeling action inherent during tensile testing of lap joint welds, the crack can open up easily and lead to premature failure. In weld ML-1 (Fig. 14B), however, there was significantly less heating (Fig. 12) to cause liquation. Furthermore, strong Mg-to-Mg metallic bonding exists at the interface between the stir zone and the bottom sheet without cracks or intermetallics. By the way, the light gray straight lines in AZ31 Mg are twin lines instead of scratches left on the sample due to poor polishing.

As compared to weld ML-3, weld ML-2 allows more of stronger Al-to-Al lap joint welding and less of weaker Al-to-Mg lap joint welding. This can explain why weld ML-2 is stronger than weld ML-3. As shown in Fig. 12 the joint strength increases in the order of ML-3, ML-2, ML-4, and ML-1. That is, weld ML-2 is stronger than weld ML-3 in spite of the higher heat input in the former.

In production, a weld such as ML-1 can be prepared as follows. 6061 Al sheets, AZ31 Mg sheets, and small AZ31 Mg sheets can be sheared with parallel edges to the predetermined width. With 6061 Al on top of AZ31 Mg and positioned, both can be clamped down simultaneously from one side. After putting the small AZ31 Mg

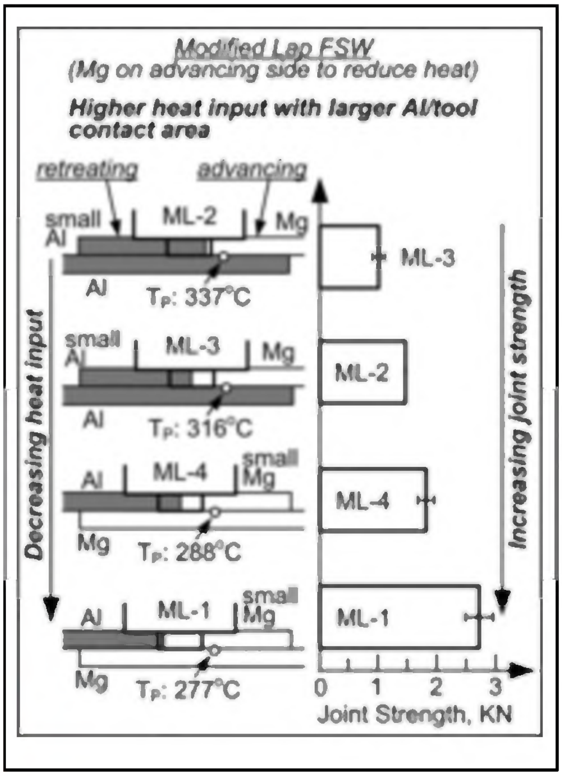

Fig. 12 — Effect of material position on joint strength and heat input in FSW of AZ31 Mg and 6061 Al in a modified lap joint. The thermocouples are 3 mm away from the path of the tool axis and 0.25 mm below the top surface of the lower sheet.

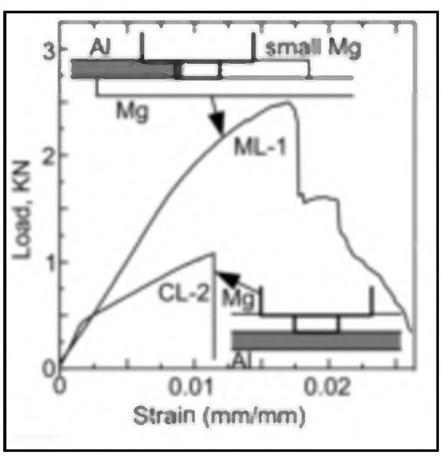

Fig. 13 — Tensile test curves of single-pass weld in conventional lap joint CL-2 and single-pass weld in modified lap joint ML-1 between AZ31 Mg and 6061 Al.

next to 6061 Al and clamping down from the opposite side, the lateral position of the joint line relative to the pin can be fine adjusted just like in butt joint welding. Since the small AZ31 Mg is free to move, its close fitup with 6061 Al is guaranteed regardless how precise the dimensions of the sheets are. The small AZ31 Mg can then be butt joint welded to 6061 Al with pin penetration into the backing plate. This, in fact, can be easier to do than ordinary butt joint FSW because pin penetration into the backing plate does not have to be carefully avoided.

Dual-Pass Weld in Lap Joint

Figure 15 shows the effect of material position on the strength of dual-pass welds in a lap joint made between AZ31 Mg and 6061 Al. For modified lap joint welds, AZ31 Mg was on the advancing side in each pass. Weld ML-6 is stronger than weld ML-7. The first pass (top) in weld ML-6 is equivalent to the single-pass weld ML-1 (Fig. 12), and that in weld ML-7 to the single-pass weld ML-4. Since weld ML-1 is stronger than weld ML-4, the first pass in the dual-pass weld can be expected to be stronger in weld ML-6 than in weld ML-7. The second pass (bottom) in weld ML-6 is equivalent to the single-pass weld ML-2 (Fig. 12), and that in weld ML-7 to the single-pass weld ML-3. Since weld ML-2 is stronger than weld ML-3, the second pass in the dual-pass weld can also be expected to be stronger in weld ML-6 than in weld ML-7.

Weld ML-6 is stronger than the dual-pass conventional lap joint weld CL-7 by a factor of about two. This significant difference is consistent with the results shown previously in Fig. 13, where the single-pass modified lap joint weld ML-1 is also about twice stronger than the single-pass conventional lap joint weld CL-2. The tensile test curves of welds CL-7 and ML-6 are shown in Fig. 16. Weld ML-6 fails at a much higher strain as well as load. Weld CL-7 failed through the weld as all other cases, but weld ML-6 failed in the 6061 Al base metal. This is the advantage of a dual-pass weld in the modified lap joint since failure in the base metal is an assurance of strong metallic bonding.

Further Discussion

How the material position affects the joint strength of the resultant weld depends significantly on how it affects the heat input and material flow during FSW, both of which affect the formation of defects and hence the joint strength. At lower travel speeds and higher rotation speeds, more heat is generated to cause liquation, and hence, cracking and intermetallic compounds to weaken the resultant weld. So, the heat input is likely to play a bigger role than material flow. At higher travel speeds and lower rotation speeds, on the other hand, less heat is generated to cause liquation. However, the materials may not be warm enough for sufficient plastic flow to keep channels from forming and weakening the resultant weld. So, material flow is likely to play a bigger role than the heat input.

In the present study, the travel speed 38 mm/min is low and the rotation speed 1400 rev/min intermediate. The results indicate that the heat input plays a bigger role than material flow in most cases. In a follow-up study much higher travel speeds are used to further examine material flow vs. the heat input.

Conclusions

Within the range of experimental conditions in the present study, the following conclusions, which can be useful for structure design in FSW of 6xxx Al to AZ or AM Mg, can be drawn:

1) Welding in a conventional lap joint of metal A at top to metal B at bottom can be modified to improve the joint strength by butt joint welding a small piece of metal B to metal A with pin penetration into the metal B at the bottom (which can be easier to do than ordinary butt joint welding because pin penetration into the backing plate is not a problem here). The highest joint strength in FSW of Al-to-Mg in the modified lap joint can double that in the conventional lap joint and match that in FSW of Mg to Mg in a lap joint. This is because similar-metal metallic bonding, which is stronger than dissimilar-metal metallic bonding, can exist over most of the interface between the stir zone and the bottom piece in a modified lap joint weld.

2) A significant effect of material position on the joint strength has been demonstrated in FSW of Al-to-Mg in butt, conventional lap, and modified lap joints, affecting the joint strength by a factor of two or more.

3) The effect of material position on the heat input has been predicted and confirmed with temperature measurements during FSW of Al-to-Mg in butt, lap, and modified lap joints. This helps better understand the effect of material position on the joint strength because a higher heat input increases the formation of liquid, and hence, cracks and brittle intermetallic compounds.

4) If the heat input is higher in FSW of A-to-A than of B-to-B under identical welding conditions, the heat input in FSW of A-to-B can be higher with A on the advancing side (in butt joint) and with a larger A/tool contact area (that is, with tool offset to A in the butt joint or with A at the top in the lap joint).

5) A three-step color etching procedure has been developed to show Mg, Al, Al_3Mg_2, and $Al_{12}Mg_{17}$ all in different col-

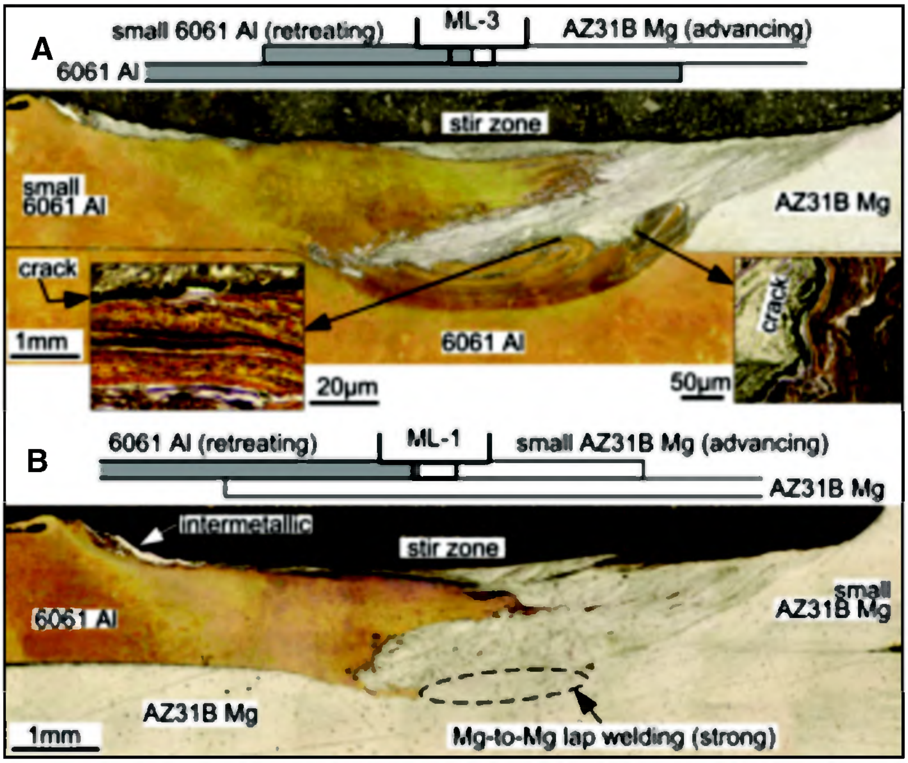

Fig. 14 — Transverse cross sections of welds in modified lap joint. A — Weld ML-3; B — weld ML-1. In B the gray straight lines in AZ31 Mg are twin lines instead of scratches from polishing.

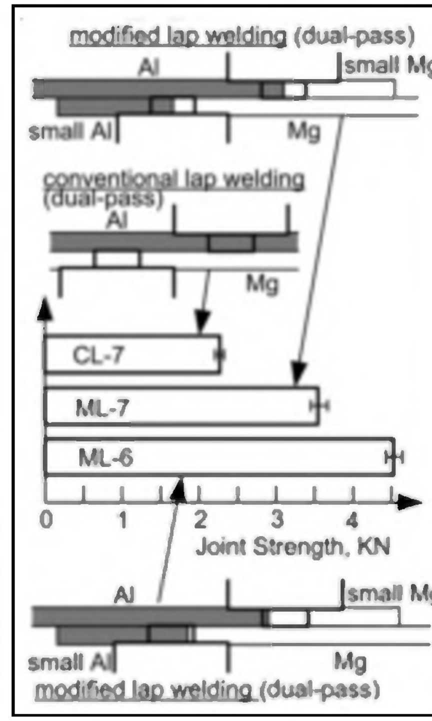

Fig. 15 — Effect of material position on strength of dual-pass welds in lap joint between AZ31 Mg and 6061 Al.

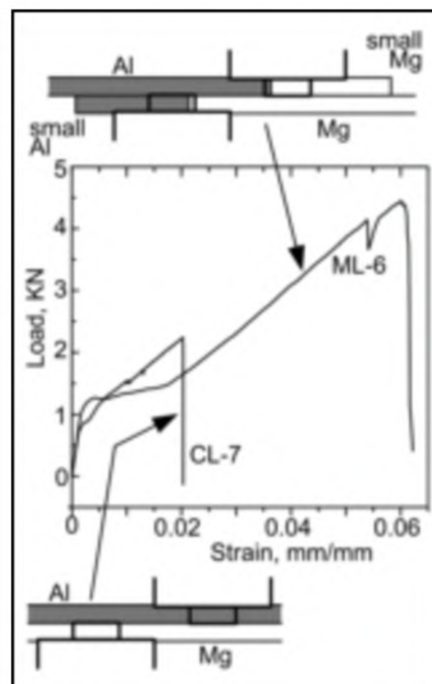

Fig. 16 — Tensile test curves of dual-pass weld CL-7 in conventional lap joint and dual-pass weld ML-6 between AZ31 Mg and 6061 Al in modified lap joint.

ors, thus enabling clear interpretation of the microstructural constituents, material flow, mixing, and evidence of liquation.

6) Material position that favors a lower heat input can be used to increase the joint strength (as long as the heat input is not too low, e.g., at high travel speeds or low rotation speeds, to maintain sufficient plastic material flow to prevent channels from forming and weakening the resultant weld).

7) In FSW of 6xxx Al to AZ or AM Mg in a butt joint the following material position favors a lower heat input: Mg on the advancing side and Al on the retreating side, with tool offset to Mg.

8) In FSW of 6xxx Al to AZ or AM Mg in a conventional lap joint the following material position favors a lower heat input: Mg on the top and Al at the bottom, with slight (e.g., 0.1 mm) pin penetration into Al.

9) In FSW of 6xxx Al to AZ or AM Mg in a modified lap joint the following material position favors a lower heat input: Mg at the bottom, Al on the top on the retreating side, and a small piece of Mg on the top on the advancing side, to which the tool offsets.

Acknowledgment

This work was supported by the Wisconsin Alumni Research Foundation (WARF) of the University of Wisconsin-Madison.

References

1. Conrardy, C. 2008. U.S. industry's top materials joining technology needs. *8th International Conference on Trends in Welding Research*, Pine Mountain, Ga., oral presentation.

2. Nakada, K., and Ushio, M. 2002. Needs and properties of dissimilar metal joining and welding. *Journal of Japan Welding Society* 71(6): 6–9.

3. Thomas, W. M., et al. 1991. Friction stir butt welding. International Patent Application No. PCT/GB92, Patent Application No. 9125978.8.

4. Chen, Y. C., and Nakata, K. 2008. Friction stir joining aluminum and magnesium alloys. *Scripta Materialia* 58: 433–436.

5. McLean, A. A., Powell, G. L. F., Brown, I. H., and Linton, V. M. 2003. Friction stir welding of magnesium alloy AZ31 to aluminum alloy 5083. *Science and Technology of Welding and Joining* 8(6): 462–464.

6. Hirano, S., Okamoto, K., Doi, M., Okamura, H., Inagaki, M., and Aono, Y. 2004. Microstructure of the interface in magnesium alloy to aluminum alloy dissimilar joints produced by friction stir welding. *Welding International* 18(9): 702–708.

7. Okamura, H., and Aota, K. 2004. Joining dissimilar materials with friction stir welding. *Welding International* 18(11): 852–860.

8. Somasekharan, A. C., and Murr, L. E. 2004. Microstructure in friction stir-welded dissimilar magnesium alloys and magnesium alloys to 6061-T6 aluminum alloy. *Materials Characterization* 52: 49–64.

9. Somasekharan, A. C., and Murr, L. E. 2006. Characterization of complex, solid-state flow and mixing in the friction-stir welding (FSW) of aluminum alloy 6061-T6 to magnesium alloy using color metallography. *Journal of Materials Science* 41: 5365–5370.

10. Sato, Y., Park, S. H. C., Michiuchi, M., and Kokawa, H. 2004. Constitutional liquation

during dissimilar friction stir welding of Al and Mg alloys. *Scripta Materialia* 50: 1233–1236.

11. Yan, J., Xu, Z., Li, Z., Li, L., and Yang, S. 2005. Microstructure characteristics and performance of dissimilar welds between magnesium alloy and aluminum formed by friction stirring. *Scripta Materialia* 53: 585–589.

12. Zettler, R., Dos Santos, J. F., Blanco, A., and da Silva, A. 2005. A study on dissimilar friction stir welds between Al and Mg alloys. *Proceedings of the 7th International Conference on Trends in Welding Research*, ASM International, pp. 413–419.

13. Zettler, R., da Silva, A. A. M., Rodrigues, S., Blanco, A., and de Santos, J. F. 2006. *Advanced Engineering Materials* 8(5): 415–421.

14. Kwon, Y. J., Shigematsu, I., and Sato, N. 2008. Dissimilar friction stir welding between magnesium and aluminum alloys. *Materials Letters* 62: 3827–3829.

15. Kostka, A., Coelho, R. S., dos Santos, J., and Pyzalla, A. R. 2009. Microstructure of friction stir welding of aluminum alloy to magnesium alloy. *Scripta Materialia*, doi: 10.1016/j.scriptamat.2009.02.020.

16. Liu, C., Chen, D. L., Bhole, S., Cao, X., and Jahazi, M. 2009. Polishing-assisted galvanic corrosion in the dissimilar friction stir welded joint of AZ31 magnesium alloy to 2024 aluminum alloy. *Materials Characterization* 60: 370–376.

17. American Society for Metals. 1986. *Binary Alloy Phase Diagrams* 1: 106, ASM International, Materials Park, Ohio.

18. Pepe, J. J., and Savage, W. F. 1967. Effects of constitutional liquation in 18-Ni maraging steel weldment. *Welding Journal* 46(9): 411-s to 422-s.

19. Pepe, J. J., and Savage, W. F. 1970. Weld heat-affected zone of the 18Ni maraging steels. *Welding Journal* 49(12): 545-s to 553-s.

20. Kou, S. 2003. *Welding Metallurgy*, 2nd edition, John Wiley and Sons, New York, N.Y., pp. 303–339.

21. Yang, Y. K., Dong, H., Cao, H., Chang, Y. A., and Kou, S. 2008. Liquation of Mg alloys in friction-stir spot welding. *Welding Journal* 87: 167-s to 177-s.

22. Nandan, R., Roy, G. G., and DebRoy, T. 2006. Numerical simulation of three-dimensional heat transfer and plastic flow during friction stir welding. *Metallurgical and Materials Transactions* A 37A: 1247–1259.

23. Nandan, R., DebRoy, T., and Bhadeshia, H. K. D. H. 2008. Recent advances in friction stir welding — process, weldment, structure and properties. *Progress in Materials Science* 53: 980–1023.

24. Cho, J. H., Boyce, D. E., and Dawson, P. R. 2005. Modeling strain hardening and texture evolution in friction stir welding of stainless steel. *Materials Science and Engineering* A 398: 146–163.

25. Cho, J. H., Boyce, D. E., and Dawson, P. R. 2007. Modelling strain hardening during friction stir welding of stainless steel. *Modelling and Simulation in Materials Science and Engineering* 15: 469–486.

26. Gerlich, A., Su, P., and North, T. H. 2005. Peak temperatures and microstructures in Al and Mg alloy FSW spot welds. *Science and Technology of Welding and Joining* 10: 647–652.

27. Su, P., Gerlich, A., North, T. H., and Bendzsak, G. J. 2006. Energy generation and stir zone dimensions in friction stir spot welding, paper 2006-01-0971, SAE International.

28. Zhang, Z., and Zhang, H. W. 2009. Numerical studies on controlling of process parameters in friction stir welding. *Journal of Materials Processing Technology* 209: 241–270.

29. Liu, X., Cui, J., Wu, X., Guo, Y., and Zhang, J. 2005. Phase growth in diffusion couples under a low frequency alternating magnetic field. *Scripta Materialia* 52: 79–82.